# Rectifying and thermocouple junctions based on Portland cement

Sihai Wen and D.D.L. Chung
*Composite Materials Research Laboratory, University at Buffalo, The State University of New York, Buffalo, New York 14260-4400*

(Received 20 July 2000; accepted 16 April 2001)

Rectifying and thermocouple junctions have been achieved using electrically dissimilar Portland cement pastes. The preferred junction is a *pn*-junction involving steel fiber cement paste (*n*-type) and carbon fiber cement paste (*p*-type). For this junction, the thermocouple sensitivity is 70 $\mu V/^{\circ}C$.

## I. INTRODUCTION

Junctions between electrically dissimilar materials are used to provide electric current rectification (as in the case of *pn*-junctions) and to provide thermocouples.

Rectifying junctions are useful as diodes for electric circuits. Various junctions can be used together to provide transistors. They are used on semiconductors, mostly commonly silicon, as the doping of a semiconductor gives *n*-type and *p*-type materials for making *pn*-junctions.

Thermocouple junctions are useful for temperature sensing. They require dissimilar materials. One example of dissimilarity is that one is *n*-type and the other is *p*-type. A thermocouple junction does not have to be a *pn*-junction, though a *pn*-junction is a junction of electrically very dissimilar materials and can serve as a relatively sensitive thermocouple junction.

The function of a thermocouple junction is based on the Seebeck effect that occurs in each of the two materials making up the junction. The more dissimilar are the two materials, the greater is the thermocouple sensitivity. Hence, the phenomenon behind a thermocouple is not an interfacial phenomenon but is associated with the difference in bulk properties between the two materials. On the other hand, the function of a rectifying junction involves an interfacial phenomenon, as the junction gives rise to a contact potential, which is key to the rectifying ability of the junction. Therefore, the quality of the interface at the junction is important to a rectifying junction but is relatively unimportant to a thermocouple junction.

Thermocouple materials are commonly metals and semiconductors with large values of the absolute thermoelectric power (i.e., large Seebeck effect). Metals are most commonly used because of their availability in the form of wires and the ease of joining metal wires by welding to form a junction.

In sharp contrast to the metals and semiconductors widely used for rectifying and thermocouple junctions, this paper uses materials based on Portland cement. Cement is a low-cost, mechanically rugged, and electrically conducting material which can be rendered *n*-type or *p*-type by the use of appropriate admixtures, such as short carbon fibers (which contribute holes) for attaining *p*-type cement and short steel fibers (which contribute electrons) for attaining *n*-type cement.[1–5] (Cement itself is weakly *n*-type in relation to electronic/ionic conduction.[1]) The fibers also improve the structural properties, such as increasing the flexural strength and toughness and decreasing the drying shrinkage.[6–13] Furthermore, cement-based junctions can be easily made by pouring the dissimilar cement mixes side by side. In addition, since cement is a structure material, cement-based junctions can be parts of a concrete structure, thereby allowing the structure to provide the rectifying and thermocouple functions. This makes the structure multifunctional and smart.

Compared to semiconductor-based junctions, cement-based junctions involve negligible materials and processing costs, as single crystals, thin films, vacuum processing, and clean rooms are not required for making cement-based junctions but are usually required for making semiconductor-based junctions. Moreover, cement-based junctions are mechanically rugged compared to semoconductor-based junctions.

## II. EXPERIMENTAL METHODS

The steel fibers used to provide strongly *n*-type cement paste were made of stainless steel No. 434, as obtained from International Steel Wool Corp. (Springfield, OH). The fibers were cut into pieces of length 5 mm prior to use in the cement paste in the amount of 0.5% by mass of cement (i.e., 0.10 vol%). The properties of the steel fibers are shown in Table I. The mechanical properties of mortars containing these fibers are described in Ref. 7. However, no aggregate, whether coarse or fine, was used in this work.

  

The carbon fibers used to provide *p*-type cement paste were isotropic pitch based, unsized, and of length approximately 5 mm, as obtained from Ashland Petroleum Co. (Ashland, KY). They were used in the amount of either 0.5% or 0.1% by mass of cement (i.e., either 0.48 or 0.96 vol% in the case of cement paste with silica fume and either 0.41 or 0.82 vol% in the case of cement paste with latex). Silica fume, due to its fine particulate nature, is particularly effective for enhancing the fiber dispersion.[14,15] The fiber properties are shown in Table II. No aggregate (fine or coarse) was used. The cement paste with carbon fibers in the amount of 1.0% by mass of cement was *p*-type, whereas that with carbon fibers in the amount of 0.5% by mass of cement was slightly *n*-type, as shown by thermoelectric power measurement.[1]

The cement used in all cases was portland cement (type I) from Lafarge Corp. (Southfield, MI). Silica fume (Elkem Materials, Inc., Pittsburgh, PA, EMS 965) was used in the amount of 15% by mass of cement. The methylcellulose, used in the amount of 0.4% by mass of cement, was from Dow Chemical Corp., Midland, MI, Methocel A15-LV. The defoamer (Colloids, Inc., Marietta, GA, 1010) used whenever methylcellulose was used was in the amount of 0.13 vol%. The latex, used in the amount of 20% by mass of cement, was a styrene butadiene copolymer (Dow Chemical Co., Midland, MI, 460NA) with the polymer making up about 48% for the dispersion and with the styrene and butadiene having a mass ratio of 66:34. The latex was used along with an antifoaming agent (Dow Corning Corp., Midland, MI, No. 2410, 0.5% by mass of latex).

A rotary mixer with a flat beater was used for mixing. Methycellulose (if applicable) was dissolved in water, and then the defoamer was added and stirred by hand for about 2 min. Latex (if applicable) was mixed with the antifoam by hand for about 1 min. Then the methylcellulose mixture (if applicable), the latex mixture (if applicable), cement, water, silica fume (if applicable), carbon fibers (if applicable), and steel fibers (if applicable) were mixed in the mixer for 5 min.

A junction between any two types of cement mix was made by pouring the two different mixes into a rectangular mold (160 × 40 × 40 mm) separately, such that the time between the two pours was 10–15 min. The two mixes were poured into two side-by-side compartments of the mold, and the paper (2-mm thick, without oil on it) separating the compartments was removed immediately after the completion of the two pours. Each compartment was roughly half the length of the entire mold.

After pouring of the mixes into oiled molds, an external electrical vibrator was used to facilitate compaction and decrease the amount of air bubbles. The resulting junction could be seen visually, due to the color difference between the two halves of a sample. The samples were demolded after 1 day and cured in air at room temperature (relative humidity = 100%) for 28 days.

Five types of cement past were prepared, namely (i) plain cement paste (weakly *n*-type, consisting of just cement and water), (ii) steel fiber cement paste (strongly *n*-type, consisting of cement, water, and steel fibers), (iii) carbon-fiber silica-fume cement paste (very weakly *n*-type, consisting of cement, water silica fume, methylcellulose, defoamer, and carbon fibers in the amount of 0.5% by mass of cement), (iv) carbon-fiber silica-fume cement paste (*p*-type, consisting of cement, water, silica fume, methylcellulose, defoamer, and carbon fibers in the amount of 1.0% by mass of cement), and (v) carbon-fiber latex cement paste (very weakly *n*-type, consisting of cement, water, latex, and carbon fibers). The water/cement ratio was 0.45 for pastes i–iv and was 0.25 for paste v. The absolute thermoelectric power of each paste is shown in Table III.[1,5]

Three pairs of cement paste were used to make junctions, as described in Table IV. For each pair, six specimens were tested in terms of the current–voltage characteristics and three specimens were tested in terms of the thermocouple behavior.

Current–voltage (*I–V*) characteristics were determined by using the two-probe method, with silver paint in conjunction with copper wires for electrical contacts. The

TABLE I. Properties of steel fibers.

| | |
|---|---|
| Nominal diameter | 60 μm |
| Tensile strength | 970 MPa |
| Tensile modulus | 200 GPa |
| Elongation at break | 3.2% |
| Volume electrical resistivity | $6 \times 10^{-5}$ Ω cm |
| Specific gravity | 7.7 g $cm^{-3}$ |

TABLE II. Properties of carbon fibers.

| | |
|---|---|
| Filament diameter | 15 ± 3 μm |
| Tensile strength | 690 MPa |
| Tensile modulus | 48 GPa |
| Elongation at break | 1.4% |
| Electrical resistivity | $3.0 \times 10^{-3}$ Ω cm |
| Specific gravity | 1.6 g $cm^{-3}$ |
| Carbon content | 98 wt% |

TABLE III. Absolute thermoelectric power (μV/°C).

| Cement paste[a] | Volume fraction fibers (%) | μV/°C | Type | Ref. |
|---|---|---|---|---|
| (i) Plain | 0 | 1.99 ± 0.03 | weakly *n* | 1 |
| (ii) $S_f$ ($0.5^b$) | 0.10 | 53.3 ± 4.8 | strongly *n* | 5 |
| (iii) $C_f$ ($0.5^b$) + SF | 0.48 | 0.89 ± 0.09 | weakly *n* | 1 |
| (iv) $C_f$ ($1.0^b$) + SF | 0.95 | −0.48 ± 0.11 | *p* | 1 |
| (v) $C_f$ ($0.5^b$) + L | 0.41 | 1.14 ± 0.05 | weakly *n* | 1 |

[a]Note: SF = silica fume; L = latex.
[b]Percent by mass of cement.

one rather than an ionic one. Moreover, the repeatability of the $I$–$V$ characteristics over time suggests that absence of any significant electrochemical reaction. Therefore, the rectification is attributed mainly to the asymmetric electron flow resulting from the *pn* or $nn^+$ junction. Due to the high concentration of electrons in the *n*- or $n^+$-side, electrons predominantly flow by diffusion from the *n*-side to the *p*-side or from the $n^+$-side to the *n*-side across the junction. This flow is enhanced by a positive voltage (i.e., forward bias), which lowers the contact potential at the junction. When the voltage is negative (i.e., reverse bias), the contact potential is high, causing the diffusion current to be low. However, electrons are swept from the *p*-side to the *n*-side or from the *n*-side to the $n^+$-side under the electric field associated with the high contact potential at the junction, resulting in a drift current in the direction opposite to the diffusion current. The drift current is enhanced by a more negative voltage but is low due to the low electron concentration in the *n*-side.

Junction b is more rectifying than junction c. This is due to the involvement of junction c with latex in the cement paste with carbon fibers and the involvement of junction b with silica fume in the cement paste with carbon fibers. As shown in Table III, silica fume (paste iii) brings out the *p*-type influence of carbon fibers more than latex (paste v). Furthermore, latex is electrically insulating and its presence at the junction may interfere with the charge transport through the junction.

The piecewise linearity in the $I$–$V$ characteristic up to +30 V in the positive voltage regime in Fig. 2 and down to −30 V in the negative voltage regime in Fig. 1, such that the slope is different between the positive and negative voltage regimes of each $I$–$V$ characteristic, is in sharp contrast to the linearity (not piecewise, but uniform, with the same slope on both sides of the origin due to ohmic behavior) range of up to +11 V and down to −11 V in the case of a homogeneous piece of cement paste without a junction (Fig. 7).[16] The origin of the piecewise linearity and slope change in the junction case (Figs. 1 and 2) is not completely clear, though it must be due to the effect of the junction on carrier movement.

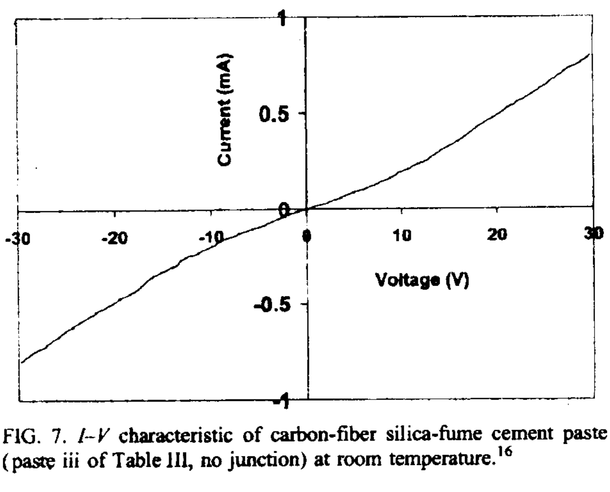


FIG. 7. $I$–$V$ characteristic of carbon-fiber silica-fume cement paste (paste iii of Table III, no junction) at room temperature.[16]

The values of the thermocouple sensitivity (Table IV) are higher than (theoretically equal to) the difference in the absolute thermoelectric power of the corresponding two cement pastes that make up the junction (Table III). For example, for junction a, the difference in the absolute thermoelectric power of pastes iv and ii is 54 $\mu$V/°C, but the thermocouple sensitivity is 70 $\mu$V/°C. The reason for this is unclear. Nevertheless, a higher thermocouple sensitivity does correlate with a greater difference in the absolute thermoelectric power.

## V. CONCLUSION

Cement-based rectifying and thermocouple junctions (*pn* or $nn^+$) have been achieved using electrically dissimilar cement pastes, such as those having different concentrations of free electrons (from steel fibers) or holes (from carbon fibers). The current from the more *p*-type or less *n*-type side to the other side of the junction is high when the voltage is positive at the former side. The current is low when the voltage is negative at the former side. The highest thermocouple sensitivity attained was 70 $\mu$V/°C. The presence of latex in the cement paste degrades the rectifying ability and thermocouple sensitivity of the junction.


## ACKNOWLEDGMENT

This work was supported in part by the National Science Foundation.


## REFERENCES


1. S. Wen and D.D.L. Chung, Cem. Concr. Res. **29,** 1989 (1999).
2. M. Sun, Z. Li, Q. Mao, and D. Shen, Cem. Concr. Res. **28,** 549 (1998).
3. M. Sun, Z. Li, Q. Mao, and D. Shen, Cem. Concr. Res. **28,** 1707 (1998).
4. M. Sun, Z. Li, Q. Mao, and D. Shen, Cem. Concr. Res. **29,** 769 (1999).
5. S. Wen and D.D.L. Chung, Cem. Concr. Res. **30,** 661 (2000).
6. P-W. Chen and D.D.L. Chung, Composites, Part B **27B,** 269 (1996).
7. P-W. Chen and D.D.L. Chung, ACI Mater. J. **93,** 129 (1996).
8. A.M. Brandt and L. Kucharska, *Materials for the New Millennium*, Proc. Mater. Eng. Conf. (ASCE, New York, 1996), Vol. 1, p. 271.
9. N. Banthia and J. Sheng, Cem. Concr. Compos. **18,** 251 (1996).
10. B. Mobasher and C.Y. Li, ACI Mater. J. **93,** 284 (1996).
11. M. Pigeon, M. Azzabi, and R. Pleau, Cem. Concr. Res. **26,** 1163 (1996).
12. N. Banthia, C. Yan, and K. Sakai, Cem. Concr. Compos. **20,** 393 (1998).
13. T. Urano, K. Murakami, Y. Mitsui, and H. Sakai, Composites, Part A **27,** 183 (1996).
14. P-W. Chen and D.D.L. Chung, J. Electron. Mater. **24,** 47 (1995).
15. P-W. Chen, X. Fu, and D.D.L. Chung, ACI Mater. J. **94,** 203 (1997).
16. S. Wen and D.D.L. Chung, Cem. Concr. Res. **29,** 961 (1999).

### B. Thermocouple behavior

Figures 4–6 show plots of the thermocouple voltage versus the temperature difference (relative to essentially room temperature) for junctions a–c, respectively. The thermocouple voltage increases monotonically and reversibly with increasing temperature difference for all junctions. The thermocouple voltage noise decreases and the thermocouple sensitivity (Table IV) and reversibility increase in the order: (c), (b), and (a). The highest thermocouple sensitivity is $70 \pm 7$ $\mu$V/°C, as attained by junction a both during heating and cooling. This value approaches that of commercial thermocouples. That junction a gives the best thermocouple behavior (in terms of sensitivity, linearity, reversibility, and signal-to-noise ratio) is due to the greatest degree of dissimilarity between the materials that make up the junction. The linearity of the plot of thermocouple voltage versus temperature difference is better during cooling than during heating for junction a.

## IV. DISCUSSION

The asymmetry in the $I$–$V$ characteristic on the two sides of the origin observed in this work for various junctions is in sharp contrast to the symmetry previously observed for a homogeneous piece of cement paste without a junction (Fig. 7).[16] This symmetry was observed for various paste compositions (pastes i, iii, and v of Table III) at various temperatures.[16] Hence, the asymmetry is attributed to the junction itself. The current at the same voltage is higher in Fig. 7 (without a junction) than in Figs. 1–3 (with a junction), due to the contact resistance associated with the junction.

Junctions a and b are rectifying, though the rectification is not perfect; the magnitude of current is much larger when the voltage is positive than when the voltage is negative. Although ionic conduction occurs in a cement phase (which contains water), the electric circuit used in obtaining the $I$–$V$ characteristics is an electronic

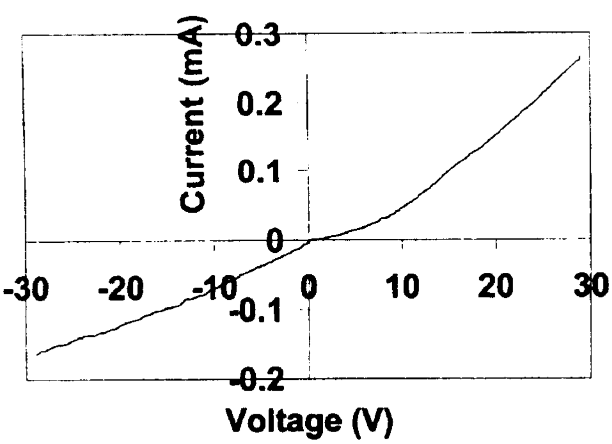


FIG. 3. $I$–$V$ characteristic of junction c of Table IV.

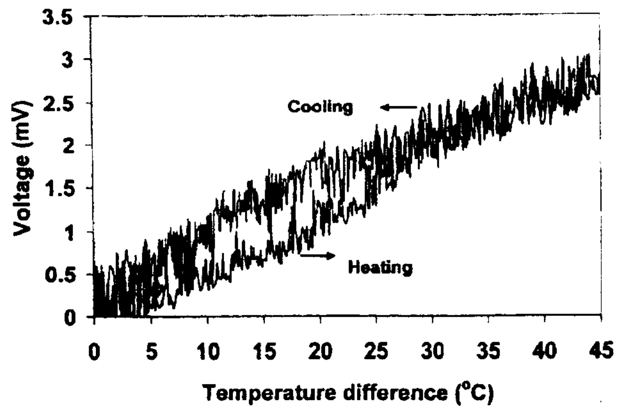


FIG. 5. Variation of the cement-based thermocouple voltage with temperature difference during heating and then cooling for junction b of Table IV.

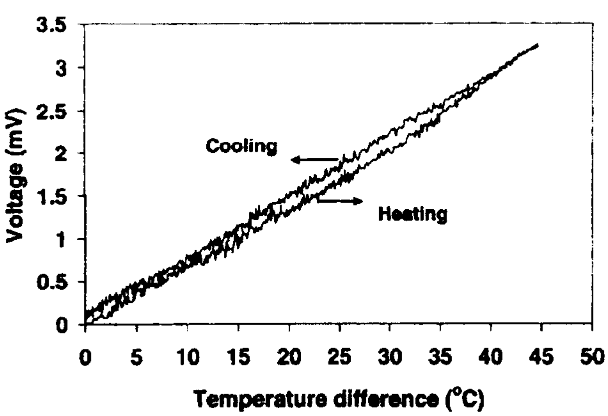


FIG. 4. Variation of the cement-based thermocouple voltage with temperature difference during heating and then cooling for junction a of Table IV.

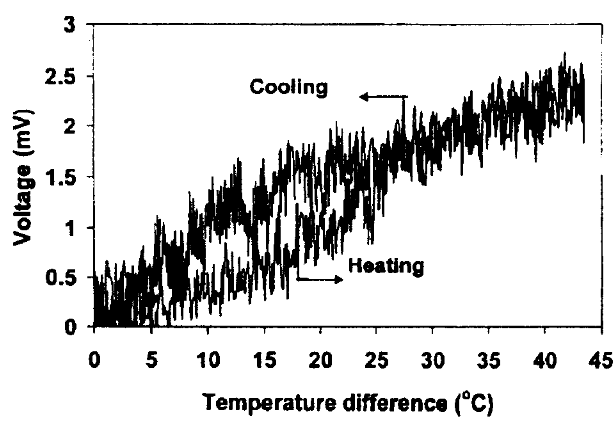


FIG. 6. Variation of the cement-based thermocouple voltage with temperature difference during heating and then cooling for junction c of Table IV.

two-probe method gave essentially the same result as the four-probe method, due to the high sample resistance. A Keithley 2001 (Cleveland, OH) multimeter was used. Each electrical contact was applied around the entire 40 × 40 nm perimeter of the rectangular specimen. The two contacts were at two parallel cross-sectional planes that were 140-mm apart, such that they were symmetrically positioned with respect to the junction. The voltage was swept from +30 to −30 V over a period of 120 s, while the current was measured. The positive end of the indicated voltage was at the first of the two listed pastes in each row in Table IV, as this is the more $p$-type or less $n$-type partner. The indicated current was in the direction from the positive end to the negative end of the indicated voltage.

Thermocouple testing was conducted by heating the junction by resistance heating, which was provided by nichrome heating wire (wound around the whole perimeter of the sample over a width of 10 mm that was centered at the junction), a transformer, and a temperature controller. The voltage difference between the two ends of a sample was measured by using electrical contacts in the form of copper wire wound around the whole perimeter of the sample at each end of the sample. Silver paint was present between the copper wire and the sample surface under the wire. The copper wires from the two ends were fed to a Keithley 2001 multimeter for voltage measurement. A T-type thermocouple was positioned to almost touch the heating wire at the junction. Another T-type thermocouple was attached to one of the two ends of the samples (at essentially room temperature). The difference in temperature between these two locations governs the voltage. Voltage and temperature measurements were done simultaneously using the multimeter, while the junction temperature was varied through resistance heating. The voltage difference divided by the temperature difference yielded the thermocouple sensitivity.

## III. RESULTS

### A. Current–voltage characteristics

Figure 1 shows the $I$–$V$ characteristic for junction a, which is a $pn$-junction. The $I$–$V$ characteristic is nonlinear within the positive voltage regime and linear within the negative voltage regime. The slope is much steeper in the positive voltage regime than the negative voltage regime. Thus, the junction is rectifying, though the rectification is not perfect and the $I$–$V$ characteristic differs in shape from that of a conventional $pn$-junction.

Figure 2 shows the $I$–$V$ characteristic of junction b, which is an $nn^+$-junction. It is similar to that in Fig. 1, except that the slope is less linear in the negative voltage regime and the current is lower at the same voltage. The lower current in Fig. 2 is consistent with the higher resistivity of cement paste iii of junction b than that of cement paste iv of junction a.

Figure 3 shows the $I$–$V$ characteristic for junction c, which is a $nn^+$-junction with less contrast between the $n$ and $n^*$ sides than the $nn^+$-junction of Fig. 2. The junction is essentially not rectifying, though the slope of the $I$–$V$ characteristic is different on the two sides of the origin. The $I$–$V$ characteristic is nonlinear.

Of all the junctions studied, only junction a is a $pn$-junction (Table IV). It gives the best rectification behavior.

TABLE IV. Cement junctions.

| Junction | Pastes involved | Junction type[a] | Thermocouple sensitivity (μV/°C) Heating | Cooling |
|---|---|---|---|---|
| a | iv and ii | $pn$ | 70 ± 7 | 70 ± 7 |
| b | iii and ii | $nn^+$ | 65 ± 5 | 65 ± 6 |
| c | v and ii | $nn^+$ | 59 ± 7 | 58 ± 5 |

[a]Note: $nn^+$ refers to a junction between a weakly $n$-type material and a strongly $n$-type material.

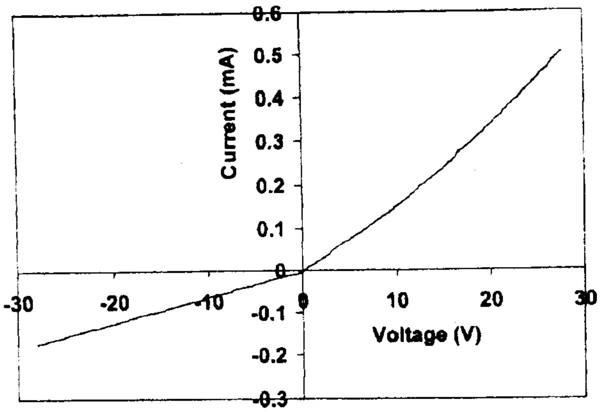


FIG. 1. $I$–$V$ characteristic of junction a of Table IV.

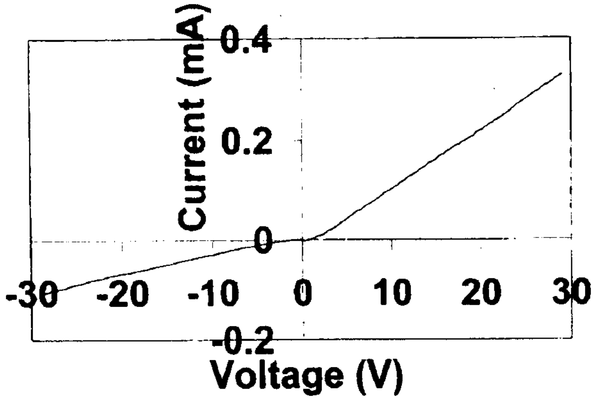


FIG. 2. $I$–$V$ characteristic of junction b of Table IV.